Tunable Single-Frequency Nd:YVO_4BiB/$_3O_6$ Ring Laser at 671 nm

Fabíola Almeida Camargo, Thomas Zanon-Willette, Thomas Badr, Niklaus Ursus Wetter, and Jean-Jacques Zondy

***Abstract*—A record of 680-mW single-frequency red emission at 671.1 nm is demonstrated using a Nd:YVO_4 ring laser intracavity frequency-doubled by a type-I critically phase-matched BiB_3O_6 crystal. Single-frequency tuning over $\Delta\lambda_{\rm red} \sim$ 1.25 nm can be achieved with a thin etalon with reflectivity of 40%. At 1342.5 nm and with a $T = 2\%$ transmission output coupler, the laser provides an optimal 1.55 W of single-frequency power.**

***Index Terms*—Intracavity second-harmonic generation, nonlinear optics, solid-state ring lasers.**

I. Introduction

A TUNABLE single-frequency solid-state laser in the visible region is desirable for high precision spectroscopic applications, as a convenient and compact alternative to continuous-wave (cw) dye lasers. In the red spectrum, for instance, the cooling transition of atomic silver or Ag ($^2S_{1/2}$–$^2P_{3/2}$) and its narrow two-photon transition ($^2S_{1/2}$–$^2D_{5/2}$), as well as the calcium (Ca) intercombination line ($^1S_0$–$^3P_1$), fall within the emission gain bandwidths of 1.32 μm ($^4F_{3/2}$–$^4I_{13/2}$) frequency-doubled σ and π-polarized Nd:YLF lasers [1], [2]. The same coincidences occur with the dipolar cooling transitions of lithium (Li) atoms ($^2S_{1/2}$–$^2P_{1/2,3/2}$) at 670.97 nm, considering a frequency-doubled Nd:YVO_4 laser at 1342 nm, which motivates this work. A laser intracavity second-harmonic generation (ICSHG) approach is the most straightforward mean to generate the required narrow-linewidth coherent sources with hundreds of mW red output power. Another advantage of solid-state lasers with respect to dye lasers are their intrinsic low frequency noise bandwidths, allowing an easier implementation of an active frequency stabilization servo with less than 50-kHz servo-control bandwidth.

Most of the works related to cw ICSHG of 1.34-μm Nd lasers, related to RGB color display lasers, employed linear standing-wave resonators and were focused on power scaling rather than spectral purity [3]–[5]. The highest cw (multi-longitudinal-mode) red output at 671 nm (3.38 W) was reported by Yao *et al.* [5], by using a double-end-pumped Nd:YVO_4/LBO laser with 27 W of diode power. Standing-wave cw lasers are difficult to operate single-frequency, especially at high-power, due to spatial hole-burning modes. Single longitudinal mode (SLM) red Nd:YVO_4 laser operation was only reported by Agnesi *et al.* [6] using a standing-wave cavity and a type II non-critically phase matched LBO crystal that served also as a birefringent etalon for hole-burning and axial mode suppression. In their experiment, stable single-frequency operation with 370 mW of red power could be maintained only by decreasing the pump power. In order to avoid spatial hole-burning modes, single-frequency lasers are most conveniently implemented using a unidirectional ring cavity configuration containing spectrally selective elements such as solid etalons for fine wavelength tuning. The presence of such lossy intracavity elements leads inevitably to a reduced output power. While multi-watt SLM 532-nm green output power can be obtained from such unidirectional ring lasers owing to the much stronger emission cross section of the $^4F_{3/2}$–$^4I_{11/2}$ transition at 1064 nm in Nd:YVO_4/LBO [7], reaching the watt-level SLM red output remains a challenge for the $\sim 4\times$ weaker emission cross section of $^4F_{3/2}$–$^4I_{13/2}$ transition at 1342 nm, which is more subject to excited-state absorption (ESA) [8].

In this work, we report on such a single-end diode-pumped Nd:YVO_4 unidirectional red ring laser containing a type-I cut BiB_3O_6 (BiBO) nonlinear crystal, yielding 680 mW of single-longitudinal mode (SLM) red output power at 671.1 nm without any intracavity etalon, owing to the self-suppression of adjacent longitudinal modes mediated by nonlinear loss competition via sum-frequency mixing [9]. This is—to the best of our knowledge—the largest cw SLM red output power ever achieved at this wavelength with an ICSHG Nd:YVO_4 laser. For smooth SLM wavelength tuning over the full gain bandwidth ($\sim$ 4 nm), a partially coated ($R = 40\%$) 100-μm-thin etalon was found necessary, reducing the maximum SLM power (at 671.15 nm) to 380 mW. When tuned to the Li atomic transition (670.97 nm), the laser could yield 200 mW of SLM power. Strategies to scale up the SLM red power to the watt-level range will be devised in the conclusion section.

II. Experimental Setup

For a single-end diode laser pumping, an asymmetric ring cavity with a total round-trip length $L_{\rm cav} = 683$ mm (corresponding to a longitudinal mode spacing ${\rm FSR}_{\rm cav} = c/L_{\rm opt} =$ 440 MHz) was used in which the AR-coated a-cut Nd:YVO_4 crystal (dimension 3 mm $\times$ 3 mm $\times$ 10 mm, from Crystech

Manuscript received July 17, 2009; revised November 17, 2009. Current version published March 03, 2010. The work of F. Almeida Camargo was supported by a Ph.D. scholarship grant from Fundação de Amparo a Pesquisa do Estado de São Paulo (FAPESP) and support from Laboratoire National de Métrologie et d'Essais (LNE).

F. Almeida Camargo and N. U. Wetter are with the Centro de Lasers e Aplicações, Instituto de Pesquisas Energéticas e Nucleares, 05508-000 São Paulo, Brazil (e-mail: facamargo@usp.br; nuwetter@ipen.br).

T. Zanon-Willette, T. Badr, and J.-J. Zondy are with the Conservatoire National des Arts et Métiers (Cnam)/Laboratoire National de Métrologie et d'Essais (LNE)/Laboratoire Commun de Métrologie LNE-Cnam, F-93210 La Plaine Saint-Denis, France (e-mail: thomas.badr@cnam.fr; jean-jacques.zondy@cnam.fr; thomas.zanon@cnam.fr).

Color versions of one or more of the figures in this paper are available online at http://ieeexplore.ieee.org.

Digital Object Identifier 10.1109/JQE.2009.2038496

Inc. Qingdao, China) is located close to one of the plane mirror M1 at the larger ring cavity waist ($w \sim 320$ μm), Fig. 1. The multiband AR-coatings of the crystal ($R < 0.2\%$ per facet at 1342 nm and $R < 2\%$ at 808 nm) were also highly transmissive at 1064 nm ($T > 85\%$) so as to suppress parasitic lasing at the stronger $^4F_{3/2}$–$^4I_{11/2}$ transition. The c axis of the vanadate host lied in the plane of Fig. 1, hence laser emission was π-polarized, a polarization configuration maximizing the emission cross section as compared with the orthogonal σ polarization [8]. The laser crystal was wrapped in an indium foil and cooled to ~ 12 °C using a thermoelectrically cooled chiller. A low-doped (0.15 at.% Nd^{3+}-doped), longer crystal ($l = 10$ mm) was preferred in order to minimize the longitudinal temperature gradient arising from the single-end pumping, resulting in a $\sim 90\%$ absorbed power from the fiber-coupled cw diode pump at 808 nm, which was focused with a waist radius $w_p \sim 260$ μm. A robust unidirectional operation was maintained using a Faraday optical diode consisting of a 20-mm-long Brewster-cut 5-mm-diameter terbium gallium garnet (TGG) rod (providing a measured $\theta \sim 7°$ polarization rotation for an axial magnetic field of $B \sim 0.4T$) followed by an AR-coated zeroth-order half-wave plate (HWP) at 1342 nm. Rotation of the HWP allowed to maximize the unidirectional output power, and also to choose the lasing direction as shown in Fig. 1. The use of a zeroth-order HWP was found crucial in maintaining a stable unidirectional lasing as the laser was tuned away from gain center. All the mirrors used for ICSHG were dichroically coated with $R > 99.8\%$ in the range 1300–1350 nm and $T \sim 90\%$ in the 650–810-nm range. Their reflectivity at 1064 nm ($R < 30\%$) was low enough to prevent any cw laser oscillation at this wavelength. All the reported ICSHG Nd:YVO_4 red lasers [3]–[6] usually employed either a type-II non-critically phase-matched (NCPM) z-cut LiB_3O_5 (LBO) as the nonlinear intracavity crystal [3], [5], [6], or a type-I critically phase-matched ($\theta = 86.1$ °C, $\varphi = 0°$) LBO [4]. Type-II cut LBO has the inconvenience to behave as a waveplate rotating the FH polarization, which may introduce some extra-loss in presence of the Brewster-cut TGG rod. The nonlinear crystal we used instead was a type-I (ooe) cut (in the xz principal plane, with $\theta = 8.6°$ and $\varphi = 0°$) BiB_3O_6 (BiBO) crystal with dimensions 5 mm $\times$ 3 mm $\times$ 10 mm (length $l_c = 10$ mm), from Crystech, Inc. BiBO is a relatively new nonlinear crystal belonging to the monoclinic borate family [10]. It possesses a much higher ($4\times$) nonlinear coefficient than LBO [2], [11], can be type-I noncritically phase-matched at room temperature along its z axis ($\theta = \varphi = 0°$) at $\lambda_\omega \sim 1150$ nm [12], but suffers from larger birefringence walkoff angle ($\rho \sim 1.4°$) than LBO ($\rho \sim 0.2°$) for type-I SHG of 1.3 μm. The BiBO crystal was dual-band AR-coated at 1.32/0.66 μm with a measured residual reflection loss of $\sim 1\%$ per facet at 1342 nm and $\sim 2\%$ at 671 nm. One of its facets was $\sim 0.2°$-wedged along the noncritical φ direction (the xz plane was perpendicular to the plane of Fig. 1). This small wedge angle was designed to finely and continuously tune the SLM wavelength over ~ 30 pm by a horizontal translation of the crystal (along its 5-mm side) without affecting the phase-matching condition, by acting on the optical pathlength of the ring cavity. Such a fine spectral tuning was necessary to probe narrow atomic transitions, since etalon-tilt tuning is discontinuous due to longitudinal mode hops. The BiBO crystal was inserted between the two curved mirrors ($R = -100$ mm), at the smaller waist of the cavity ($w_0 \sim 50$ μm). Owing to the greater sensitivity of the larger cavity waist ($w \sim 320$ μm) to slight variation (by 1–2 mm) of the distance $D \approx 115$ mm between the curved mirrors, the pump mode to cavity mode overlap was optimized by varying D via the three adjustment knobs of the mirror mount supporting one of the curved mirrors. This optimization was performed in presence of the BiBO crystal and by monitoring the red or the IR output power leaking through mirror M3. Similarly, for the FH laser experiments (i.e., without the BiBO whose refractive index is $n_c = 1.77$) the pump mode to cavity mode matching were performed in the same way, resulting in a distance D reduced by a few millimeters as compared with the ICSHG laser. For wavelength tuning, we tried two fused silica etalons: A 200-μm-thick uncoated etalon (free-spectral range $FSR_e \sim 0.5$ THz or $\Delta\lambda_\omega = 3$ nm) and a 100-μm-thick one ($FSR_e \sim 1$ THz or $\Delta\lambda_\omega = 6$ nm) with partially reflective facets ($R \sim 40\%$), both placed between the gain medium and the TGG crystal, near the larger cavity waist to minimize diffraction loss. In the case of ICSHG, part of the near-IR power leaking through M3 is used for diagnostic purposes (wavelength measurement with a ± 5 pm resolution and spectral analysis by a confocal Fabry–Pérot resonator with a $FSR = 750$ MHz free spectral range and a finesse $F \sim 100$). The initial alignment of the ring cavity was performed by forming a short (2 cm) laser cavity around the Nd:YVO_4 crystal using two plane-plane HR mirrors, and by overlapping the two counterpropagating output beams at several points of the ring resonator. This technique also facilitated the Brewster angle positioning of the TGG crystal, since the short standing-wave cavity spontaneously oscillated on the stronger π polarization. By removing the short alignment resonator, lasing of the ring resonator was easily achieved with slight tilt of one of the four cavity mirrors. The whole setup was enclosed in a Plexiglas box to protect the laser cavity from ambient air stream to reduce mode-hop events probability under SLM operation.

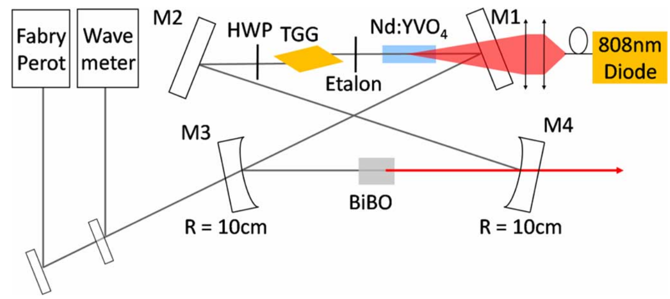

Fig. 1. Experimental setup used for an intracavity second harmonic generation of a Nd:YVO_4 laser.

III. Experimental Results and Discussions

Before investigating the ICSHG performance, we have preliminary optimized the fundamental wave (FH) output power performance of the laser by replacing M3 with partially transmitting output couplers ($T = 1\%$, 2%, and 5% at 1342 nm). The optimum output coupler was found to be $T = 2\%$ giving a

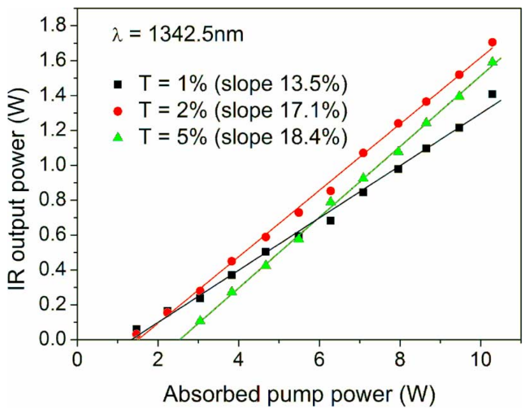

Fig. 2. Infrared output power versus absorbed pump power for different output couplers transmittance (M3), without any intracavity etalon.

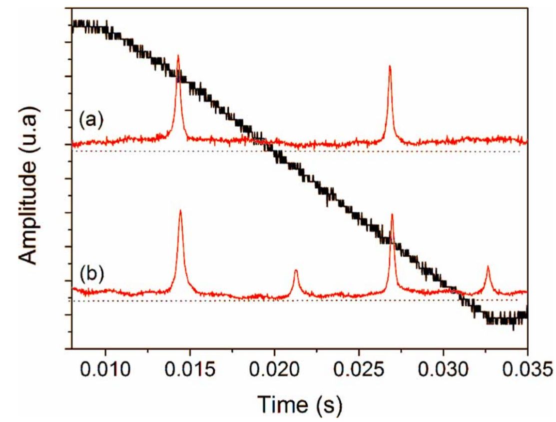

Fig. 3. Scanning confocal Fabry–Pérot spectra of the IR emission, showing SLM lasing (a) with the 40% coated thin etalon and (b) without any intracavity etalon. The scanning ramp voltage is also shown.

maximum of 1.7 W output power at an absorbed pump power of $P_{\rm abs} = 10.5$ W without any etalon (Fig. 2). From the scanning Fabry–Pérot transmission (Fig. 3), the laser oscillated on a maximum of two to three longitudinal modes around the gain center ($\lambda = 1342.3$ nm) at maximum pump power ($P_{\rm abs} \sim 10.5$ W), highlighting the advantage of a unidirectional ring cavity over a standing-wave resonator. When the absorbed power was decreased to 9.7 W, single frequency could, however, be obtained on a short time scale of a few seconds before a mode hop to an adjacent mode occurred. The optical-to-optical efficiency was 17% with a slope efficiency of 17.1%. This maximum FH power compares well with that obtained by Agnesi *et al.* from a standing-wave cavity at a similar pump power but using a higher doping level (0.5% Nd-doped) and a shorter 5-mm crystal [6]. Although we did not perform an accurate measurement of the IR beam quality factors, the inspection of the transverse pattern of the beam exiting through mirror M3 with either a viewing card or a beamscope equipped with a scanning slit revealed a nearly diffraction-limited transverse pattern. Beyond 11 W of absorbed pump power, a thermal rollover of the output power due to thermal lensing effects in the laser crystal was noticed, so that we restricted the pump power to that level. With the uncoated etalon, a stable SLM operation with a slightly reduced output power (1.55 W at maximum gain wavelength, Fig. 4) was achieved. When the 200-μm-thick uncoated etalon was replaced with the 100-μm thinner one with $R = 40\%$ facet reflectance, the SLM output power decreased further down to 1.4 W. The angular position of this thinner etalon tuned to the gain maximum was found much more inclined with respect to the cavity axis, due to the difference in their free spectral ranges, resulting in higher diffraction loss than the uncoated one. With an etalon, the FH laser could run single-frequency during half an hour without any frequency stabilization, until a mode-hop event occurred due to the slow drift of the resonator pathlength.

For the ICSHG laser, the output coupler M3 was replaced with a HR mirror and the BiBO crystal, mounted on a θ–φ–xyz positioner, was inserted in the cavity. The generated SH power was optimized by searching the optimal phase-matching angle and the optimal axial position of the BiBO with respect to the secondary waist, while subsequent

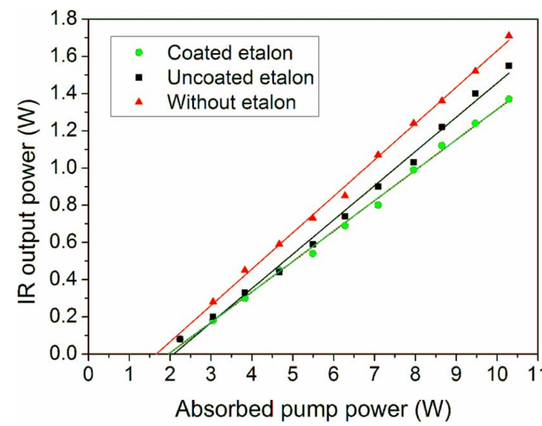

Fig. 4. FH power at 1342.3 nm versus absorbed pump power for $T = 2\%$ output coupler transmittance. The plots with etalon relate to single-frequency power.

tilts of mirrors M4 and M3 were performed to retrieve a perfect cavity alignment. With the nonlinear crystal inside the cavity, a record of 680 mW single frequency operation at gain center wavelength (671.1 nm) could be achieved without any etalon (Fig. 5) owing to the higher nonlinear loss experienced by sum-frequency processes between different longitudinal modes in a homogeneously broadened laser subject to gain saturation [7], [9]. Such a nonlinear mode discrimination mechanism works mainly with unidirectional ICSHG laser setups, because of the much reduced number of longitudinal modes competing for gain [1]. We have ascertained the role of this nonlinear mechanism by moving the BiBO in and out of the cavity: While a bi-modal spectral emission [Fig. 3(b)] was observed without the nonlinear crystal, once the latter is inserted SLM operation was instantaneously achieved [Fig. 3(a)]. The red laser was then able to oscillate on the same longitudinal mode during more than one hour before a mode-hop event occurred. This relatively stable SLM operation without any etalon is further favored by the fact that the ratio $\gamma = \Delta\lambda_{\rm NL}/\Delta\lambda_{\rm gain}$ of the nonlinear spectral bandwidth of the BiBO ($\Delta\lambda_{\rm NL} = 3.9$ nm) to the laser gain bandwidth ($\Delta\lambda_{\rm gain} \sim 3.5$ nm) is equivalent or larger than unity, a necessary condition for stable SLM operation in ICSHG lasers [13]. An intracavity etalon is, however,

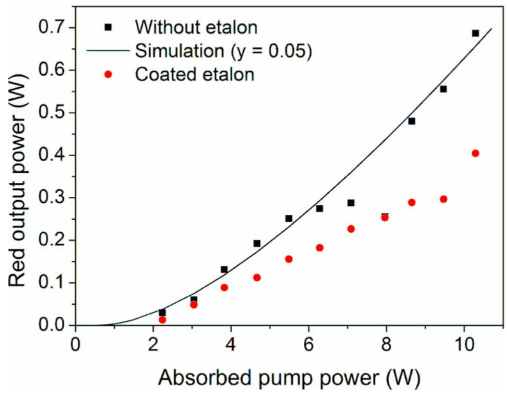

Fig. 5. Red output power versus absorbed pump power with (circles) and without (square) the $R = 40\%$ coated thin etalon. The solid line is a fit to the theoretical formula, (2).

necessary not only to prevent wavelength drift but also for tuning purpose. Long-term SLM operation at gain center with a slightly reduced red power (more than 520 mW) could be achieved with the uncoated etalon. Using the partially coated etalon, the red SLM power was reduced to 380 mW (Fig. 5, circle symbols), due to the quadratic nature of SHG process. The maximum red SLM output from this Nd:YVO$_4$/BiBO laser (680 mW) is nearly identical to the one reported for a Nd:YLF/BiBO similar ring laser [2], owing to the identical saturation intensity $I_{\rm sat} = h\nu/\sigma_{em}\tau$ (σ_{em} and τ being respectively the stimulated emission cross section and the upper state lifetime) of the 1.3 μm Nd^{3+} transitions in both hosts and the equivalent pump absorption rate [6].

The theory of single-frequency ICSHG was first addressed by Polloni and Svelto starting from the laser rate equations including quadratic nonlinear loss [14]. Two years later, Smith derived the same results for the SH power as Polloni *et al.* —but expressed with different normalized parameters—by equating the saturated (homogeneous) gain with the sum of linear and nonlinear losses [15]. Both analyses demonstrate that there is an optimal nonlinearity parameter satisfying optimal SH conversion of the fundamental laser, independently from the pumping rate. According to ICSHG theory, under optimal nonlinear coupling, the laser should yield the same harmonic power than the fundamental laser at its optimal output coupler transmission (i.e., 100% conversion efficiency). This means that our laser setup characterized by a round-trip passive linear loss $L \sim 0.03$ is capable to yield the same SLM red power as in Fig. 4, provided that a suitably high second-order nonlinearity crystal is used. In the formulation of the SH power for a four-level laser by Polloni *et al.*—that best fits our unidirectional single-frequency setup—the nondimensional nonlinear parameter is expressed as the ratio of the nonlinear loss for a circulating FF intensity $I = I_{\rm sat}$ to the linear loss L, i.e., $y = \kappa I_{\rm sat}/L$ and where the effective nonlinear coefficient (expressed in units of cm^2/W) is

$$\kappa = \left(\frac{4\pi^2}{\varepsilon c\lambda^2\omega}\right)\left(\frac{d_{\rm eff}^2}{n^3}\right)\left(\frac{l_c w}{w_0}\right)^2 G^2. \qquad (1)$$

In (1), w is the laser waist at the gain medium, w_0 the waist at the nonlinear crystal with length l_c, $d_{\rm eff}^2/n^3$ is its nonlinear figure-of-merit, c is the speed of light, and ε_0 the vacuum permittivity. The factor $G(\rho, w_0)$ accounts for the effect of walkoff and focusing (diffraction) and its expression in terms of the usual SH Gaussian beam aperture function $h(\sigma, l)$ is $G \equiv 2h/l$ [16], where $\sigma = \Delta k \cdot z_R (\Delta k = k_{2\omega} - 2k_\omega)$ is the normalized wave-vector mismatch ($z_R = (k_\omega w_0^2)/2$ is the FF beam Rayleigh length internal to the crystal) and $l = l_c/z_R$ is the focusing parameter. Let us note that contrary to Smith's formulation for a standing-wave ICSHG resonator [5], [6], [15] there is no additional multiplicative factor $2 < \beta < 4$ accounting for backward red wave interference in the definition (1) since our setup is unidirectional. Neglecting thermal effects, the SH output power for a four-level laser can then be expressed as [14]

$$P_{2\omega} = \frac{I_{\rm sat}\left(\frac{\pi w^2}{2}\right)L}{4y}\left[\sqrt{(y-1)^2 + 4yx} - (y+1)\right]^2 \qquad (2)$$

where $x = P_{\rm abs}/P_{\rm th}$ is the relative pump drive above threshold. Equation (2) has a maximum for $y_{\rm opt} = 1$ (a condition which is independent of the pump parameter x) and in this situation 100% optimal ICSHG coupling is achieved. The aperture function h for a type-I SHG is given by [16]

$$h(\sigma, l) = \frac{1}{2l}\int_{-l/2}^{l/2}\int d\tau d\tau' \frac{\exp[-\beta^2(\tau-\tau') - i\sigma(\tau-\tau')]}{(1+i\tau)(1-i\tau')} \qquad (3)$$

with $\beta = \rho/\delta_0$ being the walkoff angle scaled to the FF beam internal divergence angle $\delta_0 = \lambda_\omega/(\pi n_\omega w_0)$. For loose or plane-wave focusing ($l \to 0$), $G = 2h/l \to \mathrm{sinc}^2(\Delta k l_c/2) \approx 1$ for optimal phase-matching. The exact evaluation of the nonlinear parameter y using $d_{\rm eff}$(BiBO) = 2.5 pm/V (derived from experimental SHG efficiency measurements at 1.32 μm [2]), $w/w_0 = 6.5$, $L \approx 0.03$, $I_{\rm sat} = 6$ kW/cm^2 [6], [8], and $G = 0.30$ for $\rho = 24$ mrad and $w_0 = 50$ μm yields $y = 0.024$, far from the optimal value $y_{\rm opt} = 1$. The use of a highly nonlinear and zero-walkoff material such as periodically poled KTiOPO$_4$ (ppKTP) would yield a value approaching the optimal one while keeping a reasonable crystal length [1]. The y parameter retrieved from the best fit (with smallest χ^2 quadratic residual) of the experimental data in Fig. 5 to (2) shows indeed a moderate nonlinear coupling ($y_{\rm fit} = 0.05$) with BiBO. The fit further yields $P_{\rm th} = 0.52$ W and $I_{\rm sat}(\pi w^2/2)L = 0.10$ W.

Finally, we end with the wavelength tuning behavior of both the FF and SH lasers. Tuning was accomplished by tilting the intracavity etalon and simultaneously rotating the BiBO crystal vertically to readjust the phase-matching condition due to its smaller spectral bandwidth ($\Delta\lambda_{NL} = 3.9$ nm) compared to a quasi-noncritically phase-matched LBO for which $\Delta\lambda_{\rm NL} \approx 47$ nm [2]. In doing so, the ring cavity had to be slightly realigned to maximize the red output power. While the uncoated etalon was suited to obtain higher SLM red power near the maximum gain wavelength (~ 671.1 nm), it failed to cover the full tuning bandwidth of the emission line due to its smaller free spectral range ~ 3 nm (smaller than the gain bandwidth) and lower mode selectivity: Away from the central gain wavelength, a systematic hop to a longitudinal mode located near the etalon adjacent peak order (i.e., a jump on the other side of the gain profile) took place. For that reason we used the higher selectivity and thinner partially coated etalon

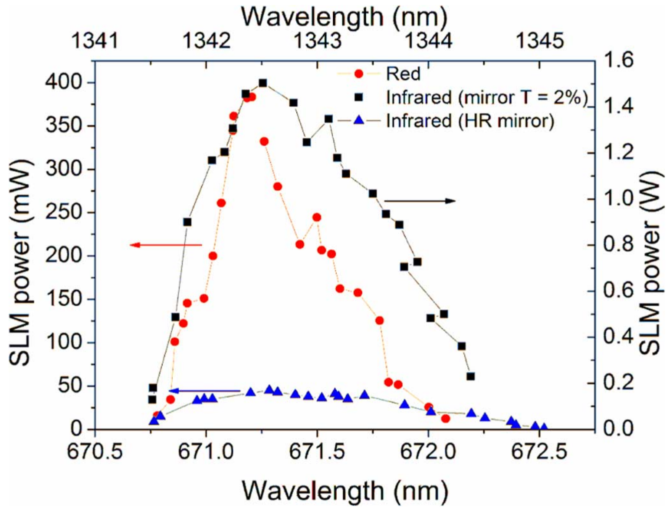

Fig. 6. Tuning curve of the red emission (circles), infrared emission when an output coupler with 2% transmission was used (squares) and infrared emission when HR mirrors were used (triangles).

despite its increased loss to achieve tuning over the full bandwidth ($\Delta\lambda_{\rm IR} \sim$ 3.5 nm) (Fig. 6). With this etalon, a smooth and continuous red tuning over nearly full gain bandwidth ($\Delta\lambda_{\rm red} \sim$ 1.25 nm) could be achieved yielding more than 380-mW SLM power at gain center (circle symbols in Fig. 6). As expected with an HR output coupler, the IR tuning range is more extended (triangle symbols) than with the 2% output coupler (square symbols). Note that the asymmetry in the tuning profiles in Fig. 6 does not reflect the actual fluorescence line shape of the transition. The steeper slope for wavelengths below the maximum gain wavelength may originate from two possible explanations: either from the increased loss of the $R = 40\%$ etalon as it was further tilted from normal incidence to cover this lower wavelength side, or to the effect of excited-state absorption (ESA) on the π-polarized stimulated emission (SE) cross section on this lower wavelength side [8, Fig. 3]. The first explanation seems quite improbable in view of the tuning lineshapes we have recorded on similar π—or—σ polarized Nd:YLF ICSHG lasers, for which the inclined etalon position did not give rise to any significant asymmetry in the tuning profiles (see, e.g., [2, Fig. 9 or Fig. 11]). The second explanation is supported by the spectroscopic data taken by Fornasier *et al.* who recorded the differential gain-ESA $\sigma_{\rm SE}-\sigma_{\rm ESA}(\lambda)$ cross section of this π-polarized 1342-nm transition in Nd:YVO_4 [8]. They found that the 1342-nm line lies exactly on several ESA transitions linking the upper $^4F_{3/2}$ level to the higher lying $^4G_{7/2}$ manifold, at 1339.5 nm. Consequently the gain-ESA spectrum in the vicinity of this transition displays an asymmetry (see their Fig. 3) similar to the one shown in Fig. 6. Due to this asymmetry, the SLM red power available at the Li ($^2S_{1/2}-^2P_{1/2,3/2}$) transition (670.97 nm) is reduced to $\sim$ 200 mW. Nevertheless, the maximum 680 mW of SLM red power reported here is the highest and narrowest ($\Delta\nu <$ 10 MHz) SLM power reported for an 671-nm ICSHG Nd:YVO_4 laser.

Lastly, let us note that the transverse beam quality of the red emission with BiBO is quite elliptical (with an ellipticity ratio $\sim 5:1$) due to the spatial walkoff dephasing effect between the driving polarization wave (o-wave) and the generated SH (e-wave) under strong type-I focusing condition [17]. The same ellipticity and astigmatism, corresponding to beam quality factors $M_x^2 = 1.33$ and $M_y^2 = 1.27$, were already observed on the red output beam (at 660.5 nm) of our previous Nd:YLF/BiBO lasers [2], in comparison with the nicer TEM_{00} red beam obtained with a walkoff-free temperature-tuned ppKTP crystal [1]. This drawback can be however circumvented with beam reshaping techniques. Alternatively, a temperature-tuned NCPM type-I (ooe) BiBO ($\theta = 0^\circ$, $\varphi = 0^\circ$) with $d_{\rm eff} \equiv -d_{12} = -2.6$ pm/V may be employed to circumvent the walkoff effect, but would require heating the crystal to a temperature $T \sim 263\ ^\circ$C as demonstrated by Peltz *et al.* [18]. Another possible choice would be a type-I (eeo) x-cut LBO ($\theta = 90^\circ$, $\varphi = 0^\circ$) cooled to $T \sim 3\ ^\circ$C to achieve NCPM, but its lower $d_{\rm eff} \equiv -d_{32} = -0.8$ pm/V would require $3\times$ longer interaction length to achieve the same conversion efficiency as a 10-mm-long NCPM BiBO.

IV. Conclusion

In conclusion, we have demonstrated up to 680-mW power in single-frequency operation at 671 nm from a cw intracavity second harmonic generation of a Nd:YVO_4/BiBO unidirectional ring laser. Unlike with linear or folded resonator standing-wave lasers [3], [6], unidirectional ring resonators can deliver SLM output up to the onset of thermal roll-over because this configuration is free of spatial hole-burning modes. In its present tunable version, the ring laser is capable to address narrow atomic resonances and hence is a challenging and cost-effective all solid-state narrow linewidth coherent source for high-resolution spectroscopy, when compared to dye lasers. With further drastic reduction of the passive intracavity loss (mainly due to the etalon and the AR-coating of the BiBO) and by using either NCPM birefringent nonlinear crystals or temperature-tuned quasi-phase-matched nonlinear crystals possessing a higher nonlinearity (such as ppKTP [1] or ppLiTaO_3 [19]), SLM red power scaling to the Watt-level range should be achievable with an optimally-coupled ICSHG ring setup and should ease wavelength tuning across the full gain bandwidth without any cavity realignment during the tuning process. The narrowness of the spectral quasi-phase-matching bandwidths associated to such periodically-poled SH converters (leading to a ratio $\gamma = \Delta\lambda_{\rm NL}/\Delta\lambda_{\rm gain} \ll 1$ and to unstable SLM operation for sufficiently long samples) can be counterbalanced with the use of a suitable intracavity etalon [1]. Finally, in order to repel the onset of thermal lensing to higher pump absorption, a double-end longitudinal pumping scheme [5] can be implemented with a six-mirror symmetric ring resonator design in which two additional dichroic plane mirrors framing the Nd:YVO_4 crystal are used to fold (in an X-shaped geometry) the M1–M2 arm in Fig. 1.

References

[1] R. Sarrouf *et al.*, "Watt-level single-frequency tunable Nd:YLF/periodically-poled $KTiOPO_4$ red laser," *Opt. Lett.*, vol. 32, pp. 2732–2734, Sep. 2007.

[2] R. Sarrouf, T. Badr, and J.-J. Zondy, "Intracavity second-harmonic generation of diode-pumped continuous-wave, single-frequency 1.3 μm Nd:$YLiF_4$ lasers," *J. Opt. A: Pure Appl. Opt.*, vol. 10, no. 104011, pp. 10–10, Aug. 2008.

[3] A. Agnesi, A. Guandalani, and G. Reali, "Efficient 671-nm pump source by intracavity doubling of a diode-pumped Nd:YVO_4 laser," *J. Opt. Soc. Amer. B, Opt. Phys.*, vol. 19, pp. 1078–1082, May 2002.

[4] H. Ogilvy *et al.*, "Efficient diode double-end-pumped Nd:YVO_4 laser operating at 1342 nm," *Opt. Express*, vol. 11, pp. 2411–2415, Sep. 2003.

[5] A. Yao *et al.*, "High-power cw 671 nm output by intracavity frequency doubling of a double-end-pumped Nd:YVO_4 laser," *Appl. Opt.*, vol. 44, pp. 7156–7160, Nov. 2005.

[6] A. Agnesi, G. C. Reali, and P. G. Gobbi, "430 mW single-transverse-mode diode-pumped Nd:YVO_4 laser at 671 nm," *IEEE J. Quantum Electron.*, vol. 34, pp. 1297–1300, Jul. 1998.

[7] Y. Zheng *et al.*, "Four watt long-term stable intracavity frequency doubling Nd:YVO_4 laser of single-frequency operation pumped by a fiber-coupled laser diode," *Appl. Opt.*, vol. 46, pp. 5336–5339, Aug. 2007.

[8] L. Fornasiero *et al.*, "Excited state absorption and stimulated emission in Nd^{3+} crystals. Part 2: YVO_4, GdVO4, and $Sr_5(PO4)_3F$," *Appl. Phys. B, Lasers Opt.*, vol. 67, pp. 549–553, Nov. 1998.

[9] K. I. Martin, W. A. Clarkson, and D. C. Hanna, "Self-suppression of axial mode-hopping by intracavity second-harmonic generation," *Opt. Lett.*, vol. 22, pp. 375–377, Mar. 1997.

[10] H. Hellwig, J. Liebertz, and L. Bohaty, "Linear optical properties of the monoclinic bismuth borate BiB_3O_6," *J. Appl. Phys.*, vol. 88, pp. 240–244, Jul. 2000.

[11] P. Tzankov and V. Petrov, "Effective second-order nonlinearity in acentric optical crystals with low symmetry," *Appl. Opt.*, vol. 44, pp. 6971–6985, Nov. 2005.

[12] M. Ghotbi and M. Ebrahim-Zadeh, "Optical second-harmonic generation properties of BiB_3O_6," *Opt. Express*, vol. 12, pp. 6002–6019, Nov. 2004.

[13] S. Greenstein and M. Rosenbluh, "The influence of nonlinear spectral bandwidth on single longitudinal mode intra-cavity second harmonic generation," *Opt. Commun.*, vol. 248, pp. 241–248, Apr. 2005.

[14] R. Polloni and O. Svelto, "Optimum coupling for intracavity second harmonic generation," *IEEE J. Quantum Electron.*, vol. QE-4, pp. 528–530, Sep. 1968.

[15] R. G. Smith, "Theory of intracavity optical second-harmonic generation," *IEEE J. Quantum Electron.*, vol. QE-6, pp. 215–223, Apr. 1970.

[16] J.-J. Zondy, D. Touahri, and O. Acef, "Absolute value of the d_{36} nonlinear coefficient of $AgGaS_2$: Prospect for a low-threshold doubly resonant oscillator-based 3:1 frequency divider," *J. Opt. Soc. Amer. B, Opt. Phys.*, vol. 14, pp. 2481–2497, Oct. 1997.

[17] J.-J. Zondy, "Comparative theory of walkoff-limited type-II versus type-I second-harmonic generation with Gaussian beams," *Opt. Commun.*, vol. 81, pp. 427–440, Mar. 1991.

[18] M. Peltz, J. Bartschke, A. Borsutzky, R. Wallenstein, S. Vernay, T. Salva, and D. Rytz, "Harmonic generation in bismuth triborate (BiB_3O_6)," *Appl. Phys. B, Lasers Opt.*, vol. 81, pp. 487–495, Aug. 2005.

[19] J. L. He *et al.*, "Generation of 840 mW of red light by frequency doubling of a 1342 nm Nd:YVO_4 laser with periodically-poled $LiTaO_3$," *Appl. Phys. B, Lasers Opt.*, vol. 74, pp. 537–539, May 2002.

Fabíola Almeida Camargo received the B.S. degree in physics from the University of São Paulo, São Paulo, Brazil, in 2003 and the M.S. degree in technology of materials from Nuclear and Energy Research Institute, São Paulo, Brazil, in 2006. She is currently working towards the Ph.D. degree on second harmonic generation in solid-state lasers, at the Lasers and Applications Center from the Nuclear and Energy Research Institute, São Paulo, Brazil.

Her main research interests are solid-state lasers and nonlinear optics.

Thomas Zanon-Willette was born in 1976. He received the Ph.D. degree in the field of atomic frequency standards based on coherent population trapping and electromagnetically induced transparency effects from the University of Pierre et Marie Curie, Paris, France, in 2005.

He spent almost two years at JILA, Boulder, CO, in the cold atoms group of J. Ye on the optical frequency standard using Strontium atoms trapped into a 1-D lattice. In 2008, he was a Lecturer at the University of Paris 13 (Laboratoire de Physique des Lasers, Villetaneuse), working in the field of chromium BEC inside a dipole trap. He is currently working on nonlinear optics and OPOs at the Laboratoire Commun de Métrologie LNE-Cnam, La Plaine Saint-Denis, France.

Thomas Badr was born in 1971. He received the Ph.D. degree in the field of lasers and high-resolution atomic spectroscopy from the University of Pierre et Marie Curie, Paris, France, in 2001.

He then joined the length metrology group at the Institut National de Métrologie (LNE-INM/CNAM), Paris, France, as a Research Engineer to work on length/frequency standards and to develop diode-pumped solid-state single-mode lasers. He is currently working on long-range laser telemetry and the optical refractometry of air.

Niklaus Ursus Wetter received the B.Sc. degree in physics from the Federal Institute of Technology of Zürich (ETHZ), Switzerland, in 1988 and the Ph.D. degree from the University of São Paulo, São Paulo, Brazil, at the Institute of Energetic and Nuclear Research in 1993.

Currently, he is a Senior Researcher and head of laser development at the Center for Lasers and Applications at IPEN-CNEN/SP, São Paulo, Brazil. His current research interests include laser design, high-power, diode-pumped lasers, and nanomaterials for the enhancement of stimulated emission.

Dr. Wetter is a member of the Brazilian Physical Society and the Optical Society of America.

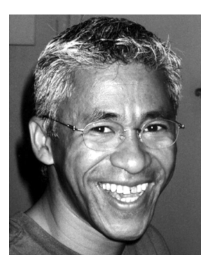

Jean-Jacques Zondy was born in Madagascar in 1959. He received the Ph.D. degree in physics from the Université de Paris-Sud, France, in 1983, in the field of lasers, atomic, and molecular physics.

In 2001, he received the title of Director of Research (HDR) from the same university. Since 1988, he has worked for the French National Bureau of Standards and got specialized in the fields of physical optics, lasers, nonlinear optics, and dynamics, high-resolution spectroscopy, and optical frequency metrology. His current research interests include nonlinear material characterization, parametric oscillators and devices, nonlinear dynamical systems, solid-state lasers, and trace gas sensing. He has published more than 100 peer-reviewed scientific papers and more than 200 conference proceedings papers.

Dr. Zondy is a member of the Optical Society of America and the European Optical Society.